Cell

Activation of Glucosidase via Stress-Induced Polymerization Rapidly Increases Active Pools of Abscisic Acid

Kwang Hee Lee,[1,2] Hai Lan Piao,[2] Ho-Youn Kim,[3] Sang Mi Choi,[1] Fan Jiang,[4] Wolfram Hartung,[4] Ildoo Hwang,[1] June M. Kwak,[5] In-Jung Lee,[3] and Inhwan Hwang[1,2,*]
[1] Division of Molecular and Life Sciences, Pohang University of Science and Technology, Pohang 790-784, Korea
[2] Center for Plant Intracellular Trafficking, Pohang University of Science and Technology, Pohang 790-784, Korea
[3] Division of Plant Biosciences, College of Agriculture and Life Sciences, Kyungpook National University, Daegu 702-701, Korea
[4] Julius-von-Sachs-Institut fur Biowissenschaften, Universitat Wurzburg, Julius-von-Sachs-Platz 2, D-97082 Wurzburg, Germany
[5] Department of Cell Biology and Molecular Genetics, University of Maryland, College Park, Maryland 20742, USA
*Contact: ihhwang@postech.ac.kr
DOI 10.1016/j.cell.2006.07.034

SUMMARY

Abscisic acid (ABA) is a phytohormone critical for plant growth, development, and adaptation to various stress conditions. Plants have to adjust ABA levels constantly to respond to changing physiological and environmental conditions. To date, the mechanisms for fine-tuning ABA levels remain elusive. Here we report that AtBG1, a β-glucosidase, hydrolyzes glucose-conjugated, biologically inactive ABA to produce active ABA. Loss of AtBG1 causes defective stomatal movement, early germination, abiotic stress-sensitive phenotypes, and lower ABA levels, whereas plants with ectopic AtBG1 accumulate higher ABA levels and display enhanced tolerance to abiotic stress. Dehydration rapidly induces polymerization of AtBG1, resulting in a 4-fold increase in enzymatic activity. Furthermore, diurnal increases in ABA levels are attributable to polymerization-mediated AtBG1 activation. We propose that the activation of inactive ABA pools by polymerized AtBG1 is a mechanism by which plants rapidly adjust ABA levels and respond to changing environmental cues.

INTRODUCTION

The phytohormone abscisic acid (ABA) plays critical roles in various physiological processes during the plant life cycle, including seed dormancy, germination, and adaptive responses to environmental stress conditions (Shinozaki and Yamaguchi-Shinozaki, 2000; Schroeder et al., 2001; Zhu, 2002; Himmelbach et al., 2003). Cellular ABA levels fluctuate constantly to allow plants to adjust to the changing physiological and environmental conditions. In particular, cellular ABA levels increase significantly during seed maturation and under abiotic stress. In contrast, ABA levels are decreased during germination (Ali-Rachedi et al., 2004; Chiwocha et al., 2005).

The primary source of ABA is de novo synthesis via complex pathways in plants (Qin and Zeevaart, 1999; Cutler and Krochko, 1999; Zeevaart, 1999; Seo and Koshiba, 2002; Nambara and Marion-Poll, 2005). Except for the final two steps, all the steps for de novo ABA synthesis occur in plastids, while the final two steps involving conversion of xanthoxin to ABA take place in the cytoplasm (Marin et al., 1996; Tan et al., 1997; Seo and Koshiba, 2002). The importance of de novo ABA synthesis in increasing ABA levels has been established using biosynthetic mutants displaying a variety of physiological defects, including precocious germination, wilting, and sensitivity to environmental stress (Rock and Zeevaart, 1991; Leon-Kloosterziel et al., 1996; Cutler and Krochko, 1999). Genes encoding biosynthetic enzymes are upregulated by physiological needs or environmental stresses, which leads to an increase in de novo ABA synthesis (Audran et al., 1998; Cutler and Krochko, 1999; Iuchi et al., 2000; Nambara and Marion-Poll, 2005).

The cellular ABA content is lowered via two pathways, hydroxylation and conjugation (Cutler and Krochko, 1999; Qin and Zeevaart, 1999; Kushiro et al., 2004). ABA is hydroxylated at three positions, C-7′, C-8′, and C-9′, of which C-8′ is the primary site. Cytochrome P450 monooxygenase hydroxylates ABA at the C-8′ position to form unstable 8′-hydroxy ABA, which is subsequently converted to phaseic acid by spontaneous isomerization. This pathway is additionally regulated by environmental conditions, such as dehydration stress (Kushiro et al., 2004). On the other hand, ABA and hydroxy ABA are conjugated with glucose for inactivation. Of the conjugates, ABA glucose ester (ABA-GE) is the predominant form (Cutler and Krochko, 1999). ABA glucosyltransferase performs the conjugation (Xu et al., 2002). In specific tissues,

conjugation presents a major pathway of ABA inactivation (Cutler and Krochko, 1999; Zeevaart, 1999). Conjugated ABA-GEs are compartmentalized in vacuoles or apoplastic space (Dietz et al., 2000). However, the issue of whether biologically inactive ABA-GEs constitute a reserved or stored form of ABA remains to be clarified.

Despite recent progress in research on ABA metabolism, the mechanisms by which the ABA content is regulated at the cellular and whole plant levels are currently unclear. De novo synthesis is essential to increase the cellular ABA content. In addition, at the whole plant level, ABA is transported from roots to leaves by long-distance translocation (Wilkinson and Davies, 2002). Thus, the cellular ABA level in a leaf cell may be increased by two different sources, specifically, de novo synthesis in the leaf cell and supply from roots. Furthermore, ABA-GE may contribute to ABA homeostasis in plant cells (Hartung et al., 2002; Sauter et al., 2002; Chiwocha et al., 2005).

In this study, we demonstrate that AtBG1, an *Arabidopsis* β-glucosidase homolog localized to the ER, displays ABA-GE hydrolyzing activity, and increases the cellular ABA content through rapid polymerization of AtBG1 from lower to higher molecular weight forms under dehydration stress.

RESULTS

The *atbg1* Mutant Displays ABA-Deficient Phenotypes

We isolated *AtBG1* (see Figure S1 in the Supplemental Data) encoding a β-glucosidase homolog as an NaCl-inducible gene from an *Arabidopsis* subtraction library enriched for NaCl-stress-inducible cDNA (Pih et al., 1997). *AtBG1* expression was induced in leaves under various abiotic stress conditions and following exposure to exogenous ABA (Figure S2A). To further determine the expression pattern, the *AtBG1* upstream region was placed in front of the β-glucuronidase (GUS) coding region, and the resulting construct was introduced into plants. GUS expression was detected in seed cells. In vegetative tissues, GUS expression was low and highly specific to hydathodes of rosette and cauline leaves (Figures S2B and S2C). Dehydration stress strongly induced GUS expression in hydathodes and the vasculature of rosette and cauline leaves, suggesting that AtBG1 participates in drought response (Figure S2C). To test this hypothesis, we generated transgenic plants harboring *AtBG1* under control of the cauliflower mosaic virus (*CaMV*) *35S* promoter (Figure S3A). Transgenic plants exhibited enhanced tolerance to NaCl stress, supporting our hypothesis (Figure S3B).

Next, a mutant line with a T-DNA insertion in the ninth intron of *AtBG1* was isolated (see Figure S4), and the absence of *AtBG1* mRNA was confirmed by RT-PCR (Figure 1A). Homozygous mutant plants were smaller, and displayed a yellow leaf phenotype (Figures 1C and 1D), defective stomatal closure in the dark (Figure 1F), increased transpirational water loss (Figure 1G), and sensitive response to dehydration (Figure 1H), indicating that loss of *AtBG1* leads to defects in ABA-mediated responses. In addition, *atbg2* plants, which had a T-DNA insertion in *AtBG2*, encoding another β-glucosidase with ABA-GE hydrolyzing activity, displayed similar but weaker phenotypes to those of *atbg1* plants (K.H.L., J.C. Jeong, D.-J. Yun., and I.H., unpublished data). Furthermore, application of exogenous ABA to *atbg1* plants rescued the defect in stomatal movement and plant growth phenotypes (Figures 1E and 1F). In fact, the ABA levels in *atbg1* plants were lower than the wild-type (WT) (see below Figure 4 for detail). To confirm that these phenotypes were due to the T-DNA insertion in *AtBG1*, genetic complementation was performed by expressing an epitope hemagglutinin (HA)-tagged *AtBG1* cDNA (*AtBG1:HA*, Figure S4C) under the control of the *CaMV 35S* promoters in the *atbg1* background. Expression of AtBG1:HA in rescued plants was confirmed by western blot analysis of protein extracts from the T2 generation using an anti-HA antibody (Figure 1B). Expression of AtBG1:HA rescued the mutant phenotypes (Figures 1C, 1D and 1F–1H). To further confirm the complementation, *atbg1* mutants were transformed with *AtBG1:HA* under the *AtBG1* promoter (Figure 1C, Rescued *atbg1-E*). There was no difference between the two rescued plant phenotypes, and all following analyses were performed with *atbg1* plants rescued with *AtBG1:HA* under the *CaMV 35S* promoter.

AtBG1 Exhibits ABA-GE Hydrolyzing Activity In Vitro

To elucidate the mechanistic basis of the mutant phenotype described above, we assessed the enzymatic activity of AtBG1. We examined the possibility that AtBG1 hydrolyzes ABA-GE, an irreversible and sequestered form of ABA in plants (Zeevaart, 1999; Seo and Koshiba, 2002). Protoplasts were transformed with *AtBG1:HA*, *AtBG1[E207Q]:HA*, *AtBG1[ΔC105]:HA*, or a vector control. AtBG1[E207Q]:HA contains a substitution at position 207, which is part of the active site of various β-glucosidases (Marana et al., 2001). AtBG1[ΔC105] is a deletion mutant that lacks 105 residues at the C terminus. Transiently expressed proteins in protoplasts were immunopurified from protein extracts prepared 24 hr after transformation using an anti-HA antibody (Figure 2A). Immunopurified proteins were incubated with ABA-GE in vitro, and the reaction products were separated by high-pressure liquid chromatography (HPLC). Both AtBG1:HA and AtBG1[E207Q]:HA displayed a novel peak at the position for ABA, which was smaller in the latter case (Figure 2B). The putative ABA peak was further confirmed and quantified by enzyme-linked immunosorbent assay (ELISA) using an antibody that specifically recognizes ABA, but not ABA-GE (Xu et al., 2002). The amount of ABA released by AtBG1[E207Q]:HA was reduced to 25% of that of the WT (Figure 2C), indicating that glutamic acid at position 207 is important for hydrolytic activity. However, neither AtBG1[ΔC105]:HA nor the vector control generated detectable levels of ABA from ABA-GE (Figures 2B and 2C). Together, these results clearly demonstrate that AtBG1:HA hydrolyzes ABA-GE to ABA. Zeatin-GE

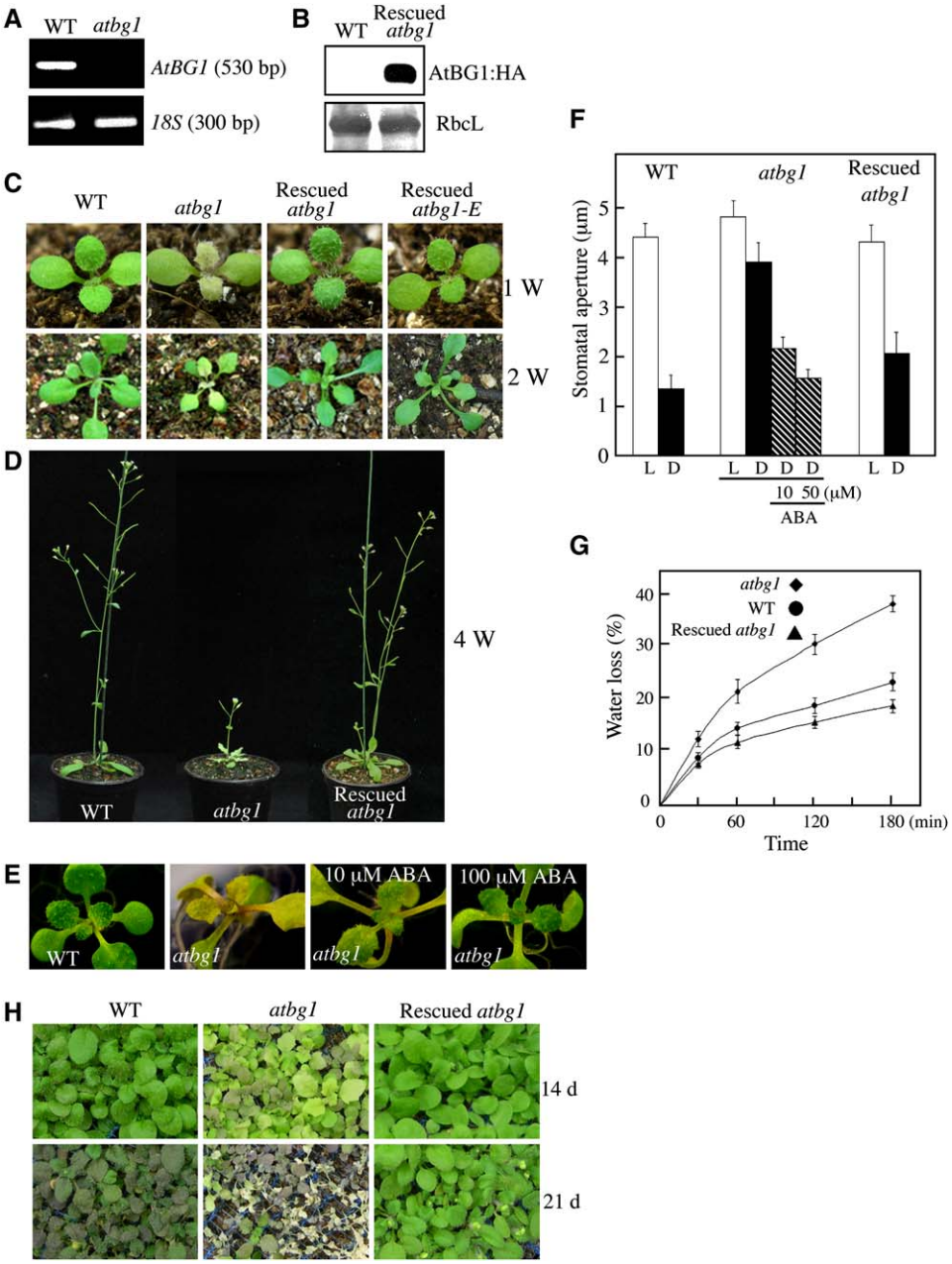

Figure 1. Phenotypes of *atbg1* Mutants and Complementation with *AtBG1:HA*

(A) Lack of *AtBG1* transcripts in *atbg1* plants was confirmed by RT-PCR using gene-specific primers. 18S rRNA indicates a positive control for RT-PCR.

(B) AtBG1:HA expression in rescued *atbg1* plants was determined by western blotting using an anti-HA antibody.

(C and D) WT, *atbg1*, and rescued *atbg1* plants grown on soil for 1 (1 W), 2 (2 W), and 4 (4 W) weeks after germination. Rescued *atbg1* and Rescued *atbg1*-E indicate *atbg1* plants harboring *CaMV 35S-AtBG1:HA* and *AtBG1p-AtBG1:HA*, respectively.

(E) *atbg1* mutants were rescued by exogenous ABA. One-week-old *atbg1* plants were treated with ABA, and grown for an additional 3 days.

(F) Stomatal aperture was measured with and without exogenously applied ABA at 12 hr (L) and 23 hr (D) (n = 150). Error bars = standard deviation (SD).

(G) The *atbg1* plants displayed increased transpirational water loss. Detached rosette leaves (50 leaves) were exposed to 30% (v/v) RH for the indicated periods, and fresh leaf weights were measured (n = 5). Water loss is expressed as a percentage of initial fresh weight. Error bars = SD.

(H) WT, *atbg1*, and rescued *atbg1* plants were grown on soil, and not watered for 14 days (14 d) or 21 days (21 d) in a greenhouse at 20°C with 70% RH.

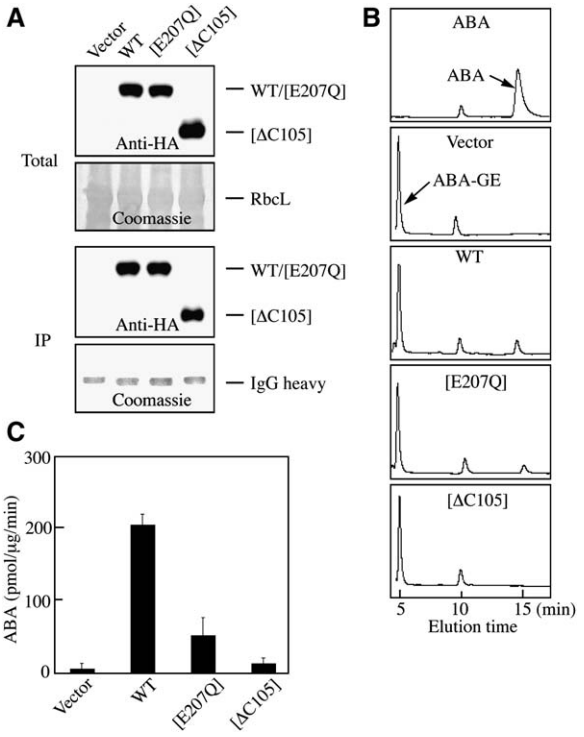

Figure 2. Hydrolysis of ABA-GE by AtBG1

(A) *AtBG1:HA, AtBG1[E207Q]:HA*, and *AtBG1[ΔC105]:HA* were expressed in protoplasts and analyzed by western blotting using an anti-HA antibody. These proteins were purified by immunoprecipitation using an anti-HA antibody. Vector indicates the empty vector used as a negative control.

(B) Immunopurified AtBG1:HA proteins were incubated with ABA-GE in vitro, and the reaction products were separated by HPLC.

(C) Putative ABA fractions of HPLC were analyzed by ELISA using an anti-ABA antibody. Error bars = SD (n = 3).

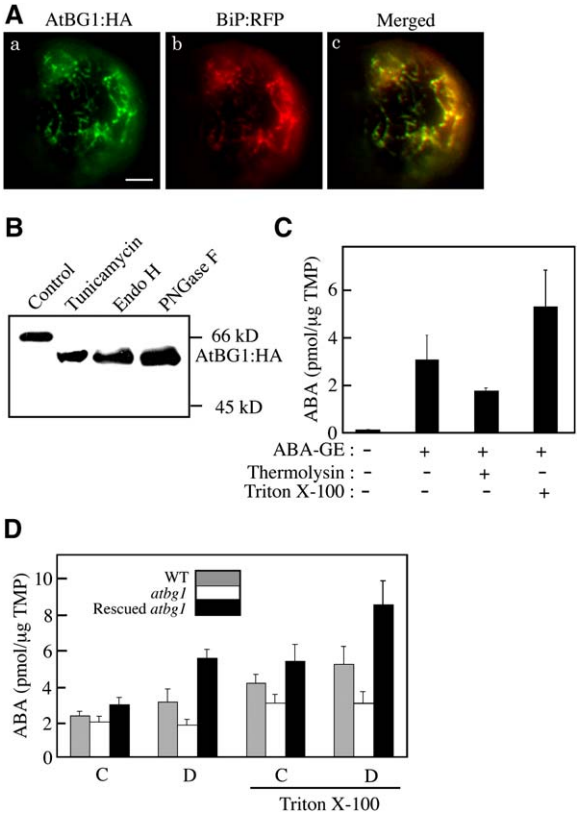

Figure 3. ER-Localized AtBG1 Hydrolyzes ABA-GE to ABA

(A) Protoplasts from rescued *atbg1* plants (line 4) were transformed with *BiP:RFP*. AtBG1:HA was detected by immunostaining with an anti-HA antibody. RFP was observed directly. Scale bar, 20 μm.

(B) AtBG1:HA contains endo H- and PNGase F-sensitive glycans. Protein extracts were treated with endo H and PNGase F as described in the Experimental Procedures. The control represents protein extracts from protoplasts in the absence of tunicamycin.

(C) ABA production by microsomal fractions in vitro. Microsomal fractions were prepared from rescued *atbg1* plants (line 4) by ultracentrifugation. The microsomal fraction was further treated with either 1% Triton X-100 or thermolysin (10 μg/ml). Error bars = SD (n = 5). TMP, total microsomal protein.

(D) ABA-GE hydrolyzing activity was measured in microsomal fractions from WT, *atbg1*, and rescued *atbg1* plants (line 4). For dehydration stress, plants were exposed to 30% RH for 10 hr. C, control; D, dehydration. Error bars = SD (n = 5; p = 0.092 between *atbg1* and WT in control samples without dehydration; $p < 0.05$ for the rest of the samples). TMP, total microsomal protein.

was incubated with AtBG1 to determine its specificity. Under our experimental conditions, AtBG1 did not exhibit hydrolytic activity on zeatin-GE (data not shown), suggesting that the enzyme is specific for ABA-GE.

AtBG1 Localizes to the ER, Where It Hydrolyzes ABA-GE to Form Free ABA

To determine the site of ABA production from ABA-GE, we examined subcellular localization of AtBG1. AtBG1 contains a sequence motif at the C terminus, REEL, which is similar to the ER retention signal KDEL (Munro and Pelham, 1987). Localization of AtBG1:HA (Figure S4C) in transgenic plants was examined immunohistochemically using the anti-HA antibody. AtBG1:HA displayed a network pattern closely overlapping that of BiP:RFP, an ER marker protein (Figure 3A) (Jin et al., 2001). GFP:AtBG1 transiently expressed in protoplasts also exhibited a network pattern closely overlapping BiP:RFP (Figures S5A and S5B), further confirming that AtBG1 localizes to the ER. To obtain independent evidence for the localization, we examined AtBG1:HA glycosylation. Proteins that localize to the ER, but not the Golgi or post-Golgi compartments, have endo H- and PNGase F-sensitive glycans (Kuznetsov et al., 1993). Protein extracts were prepared from transformed protoplasts in the presence and absence of tunicamycin, an inhibitor of N-glycosylation, and treated with endo H or PNGase F. AtBG1:HA from tunicamycin-treated protoplasts migrated faster than that from tunicamycin-untreated protoplasts (Figure 3B), indicating that AtBG1:HA is glycosylated. Furthermore, the glycan moiety of AtBG1:HA is sensitive to both endo H and PNGase F, as reflected by its higher mobility,

compared with untreated AtBG1:HA (Figure 3B), further supporting its localization to the ER.

Next, we examined whether ER-localized AtBG1:HA hydrolyzes ABA-GE. ABA-GE hydrolyzing activities were examined in microsomal fractions obtained from rescued *atbg1* plants (Figure S6A). The microsomal fraction that remained intact during an in vitro assay (Figure S6B) produced ABA from exogenously added ABA-GE (Figure 3C). The ABA-producing activity was significantly higher in the presence of Triton X-100 (Figure 3C), suggesting that ABA-GE with limited membrane permeability (Baier et al., 1988) is imported into the ER by a membrane-localized transporter. To confirm this hypothesis, we prepared thermolysin-treated microsomes and measured ABA production. The specific degradation of membrane proteins and not lumenal proteins by thermolysin was confirmed from the differential sensitivities of AtERD2:GFP and AtBG1:HA to thermolysin (Figure S6C). Thermolysin treatment induced a 40% decrease in ABA production (Figure 3C), implying that ABA-GE is imported into the ER by a transporter. The remaining 60% activity is possibly due to incomplete digestion of the putative transporter by thermolysin (Figure S6C). To further confirm these results, the ABA-GE hydrolyzing activity was measured in microsomes from *atbg1* and rescued *atbg1* plants. *atbg1* and rescued *atbg1* plants showed lower and higher ABA-GE hydrolyzing activities than the WT, respectively (Figure 3D). The difference was more pronounced when plants were subjected to dehydration stress (Figure 3D). Additionally, we prepared intracellular and extracellular protein fractions from leaf tissues (Dietz et al., 2000) and measured the ABA-GE hydrolyzing activity in each fraction. The extracellular levels of ABA-GE hydrolyzing activity in *atbg1* and rescued *atbg1* plants were similar to that in the WT (Figure S7). In contrast, the intracellular activities of *atbg1* and rescued *atgb1* plants were 50% and 160% of the WT, respectively, indicating that AtBG1 is responsible for intracellular ABA-GE hydrolysis (Figure S7). The remaining 50% of the intracellular activity in *atbg1* plants may be due to another β-glucosidase homolog that can hydrolyze ABA-GE (K.H.L., J.C. Jeong, D.-J. Yun., and I.H., unpublished data). The significantly increased activity in rescued *atbg1* plants is possibly due to the high level of AtBG1:HA expression induced by the *CaMV 35S* promoter.

AtBG1 Contributes to Increased Cellular ABA Levels under Dehydration Conditions

To determine whether there is a correlation between the ABA-GE hydrolyzing activity and the ABA level in plants, we measured the ABA content in seeds, leaves, and roots of WT, *atbg1*, and rescued *atbg1* plants by ELISA using an anti-ABA antibody. In addition, the ABA levels in representative samples were confirmed by gas chromatography-mass spectroscopy (GC-MS) (Figures S8 and S9A). The ABA content in *atbg1* seeds was approximately 40% of the WT (Figure 4A). In rescued *atbg1* plants, the ABA content ranged from 86% to 250% of the WT, which correlated positively with the levels of AtBG1:HA (Figure 4B).

Because ABA levels increase significantly under stress conditions (Zeevaart, 1999), we determined the ABA levels in leaves under both water-sufficient and dehydration conditions to establish whether AtBG1 plays a role in stress responses. Under water-sufficient conditions, the ABA content in leaves of *atbg1* and rescued *atbg1* plants was 90% and 110% of the WT, respectively (Figure 4C and Figure S9B), indicating that ABA levels do not differ significantly in all three plants under water-sufficient growth conditions. In contrast, during dehydration, ABA levels increased in all three plants, but at different extents, depending on the AtBG1 expression level. The ABA content increased 4-, 5-, and 20-fold in *atbg1*, WT, and rescued *atbg1*, respectively (Figure 4C and Figure S9B), showing that AtBG1 contributes a notable increase in ABA content upon dehydration stress. Earlier studies show that the de novo synthesis of ABA contributes to dehydration-induced increase in ABA levels (Qin and Zeevaart, 1999; Cutler and Krochko, 1999). Thus, to further determine the contribution of AtBG1, the ABA contents were measured in the presence of fluridone, an inhibitor of de novo ABA biosynthesis (Gamble and Mullet, 1986). In the presence of fluridone, ABA contents in dehydration-stressed *atbg1*, WT, and rescued *atbg1* plants were 3-, 4-, and 8-fold of the WT grown under water-sufficient conditions in the absence of fluridone, respectively (Figure 4C), indicating that dehydration stress also caused an increase in ABA content in all three plants, but to a lesser degree, compared with that in the absence of fluridone. Dehydration-induced increases in ABA levels upon fluridone addition were strongly dependent on AtBG1 expression in plants. These results strongly suggest that AtBG1 increases the ABA content upon dehydration in the absence of de novo ABA synthesis. However, upon treatment with fluridone, the amount of ABA produced in rescued *atbg1* plants during dehydration stress was increased by 8-fold, in contrast to 20-fold in the absence of fluridone (Figure 4C), suggesting that ABA generation by AtBG1 also depends on de novo synthesis. Similar results were obtained with roots, although the difference of ABA contents in the roots of these plants was smaller than that in the leaves (Figure S10). To confirm the differences in ABA contents of these plants, germination was examined. The germination rates of these plants were exactly the inverse of the ABA levels (Figures 4A and 4D). These data further support the view that ABA produced by AtBG1 plays a critical role in physiological responses in plants.

ABA-GE Hydrolyzing Activity of AtBG1 Is Enhanced by Dehydration Stress-Induced Polymerization

In rescued *atbg1* plants expressing AtBG1:HA under the control of the constitutive *CaMV 35S* promoter, the substantial increase in ABA contents required dehydration stress. This result strongly suggests that AtBG1 is activated by dehydration, leading to enhanced ABA production. We investigated the mechanism by which dehydration stress activates AtBG1. A previous study shows

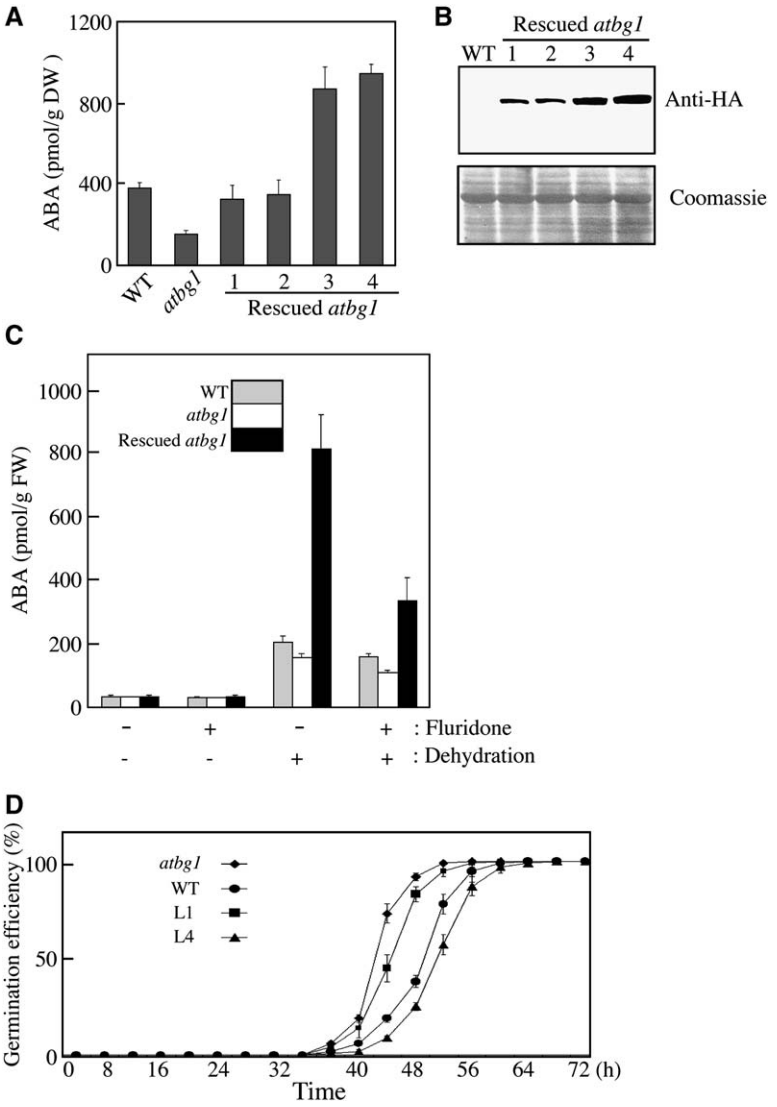

Figure 4. Endogenous ABA Levels in Seeds and Leaf Tissues

(A) ABA levels in seeds of WT, *atbg1*, and rescued *atbg1* plants were measured as described in the Experimental Procedures. Error bars = SD (n = 3).

(B) Expression of AtBG1:HA in rescued *atbg1* plants (line 1 to line 4) was analyzed by western blotting using an anti-HA antibody. The membrane was stained with Coomassie blue to control loading.

(C) ABA levels in leaves of WT, *atbg1*, and rescued *atbg1* plants (line 4) were measured. For fluridone treatment, plants grown on MS plates for 20 days were transferred onto MS plates supplemented with 1.0 μM fluridone, and cultured for additional 2 days. For dehydration stress, plants grown with or without fluridone were exposed to 30% RH for 10 hr. Error bars = SD (n = 3).

(D) Germination assays were performed with WT, *atbg1*, and rescued *atbg1* (line 1 and line 4) plants. For each plant line, 200 seeds were used in a triplicate experiment. Error bars = SD (n = 3).

that polymerized forms of β-glucosidases have higher enzymatic activity (Kim and Kim, 1998). To determine whether this is a possibility for AtBG1, we initially examined homomeric interaction of AtBG1 molecules by coimmunoprecipitation. Protein extracts from protoplasts cotransformed with two differently tagged forms of *AtBG1*, *AtBG1:HA* and *AtBG1:T7*, were used for immunoprecipitation with anti-T7 antibody. Immunoprecipitates were analyzed by western blotting using an anti-HA antibody. AtBG1:HA was detected in the precipitate (Figure S11A). Furthermore, the amount of AtBG1:HA in the precipitate was increased by 3-fold upon treatment of protoplasts with PEG 8000, a chemical that induces osmotic stress (Figure S11A). Thus, we concluded that AtBG1 undergoes homomeric interactions, which are enhanced by osmotic stress. To further address this possibility, protein extracts from rescued *atbg1* plants that had been subjected or not to dehydration stress were fractionated using a gel filtration column. Protein fractions were analyzed by western blotting using an anti-HA antibody. AtBG1:HA from unstressed plants existed primarily as monomers or dimers with a small proportion of higher molecular weight forms (Figure 5A). In contrast, AtBG1:HA from dehydration-stressed plants existed as higher molecular weight forms with almost no dimers or monomers (Figure 5A). The molecular weight of the main peak of AtBG1 in dehydration-stressed plants corresponded to over 600 kDa, which is equivalent to a 10-mer. The total amount of AtBG1:HA in stressed plants was nearly the same as that of the control (Figure S11B). Our data clearly imply that dehydration induces polymerization of AtBG1.

The enzymatic activities of high and low molecular weight forms were compared. High molecular weight forms exhibited 4-fold higher specific activity than the low molecular weight forms (Figure 5B). In addition, we measured the ABA-GE hydrolyzing activity after mixing the fractions containing high and low molecular weight forms. From these experiments we did not find any

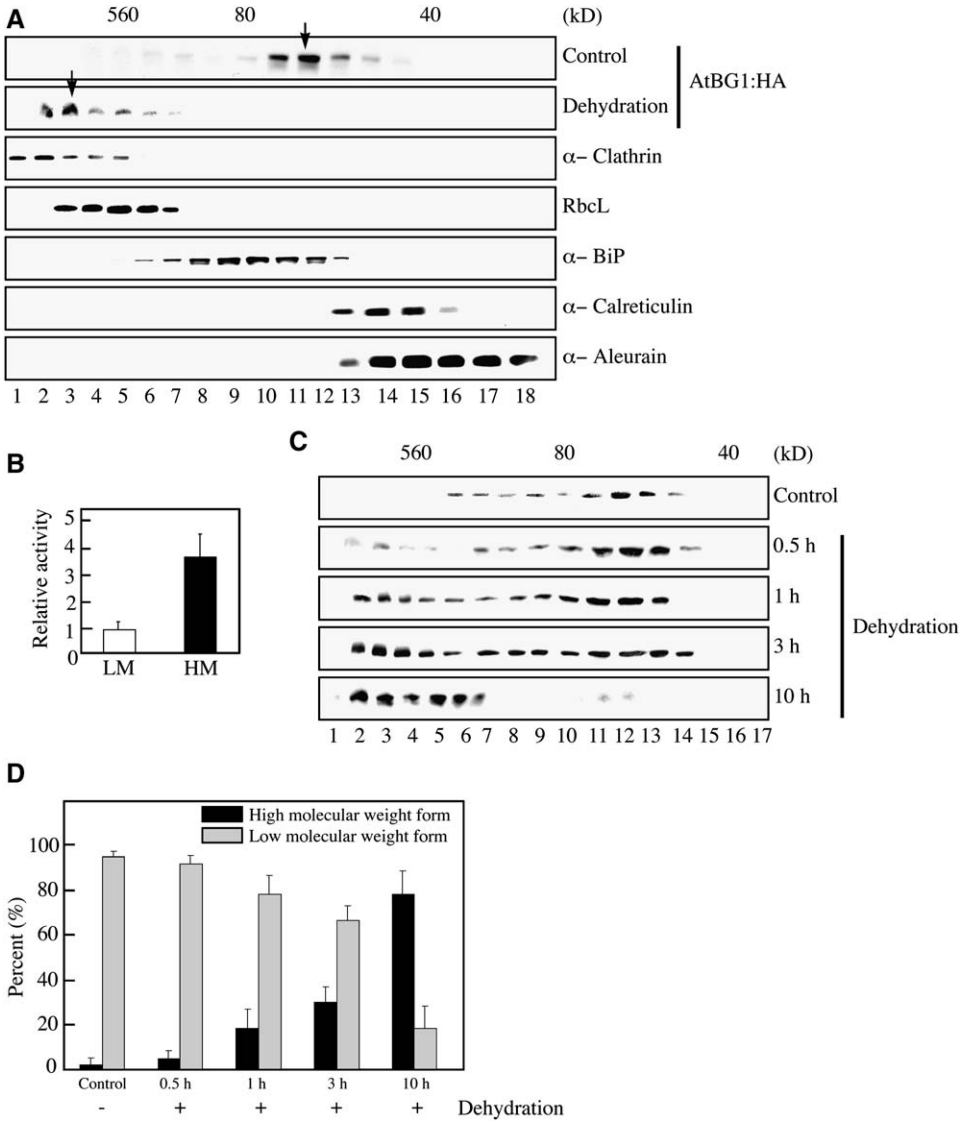

Figure 5. Dehydration Enhances the ABA-GE Hydrolyzing Activity of AtBG1 in Microsomes by Rapid Polymerization of AtBG1 into High Molecular Weight Forms

(A) Polymerization of AtBG1. Rescued *atbg1* plants were grown on MS plates for 3 weeks. For dehydration stress, plants were exposed to 30% RH for 10 hr. Protein extracts were fractionated using a gel filtration column. The fractions were analyzed by western blotting using an anti-HA antibody. The molecular weight positions were determined by western blot analysis using the indicated antibodies.

(B) ABA-GE hydrolyzing activity of lower and higher molecular weight AtBG1. Fractions indicated by arrows in Figure 5A were assayed for ABA-GE hydrolyzing activity in vitro. The activity was normalized based on the intensity of AtBG1:HA bands detected by an anti-HA antibody. LM, low molecular weight form; HM, high molecular weight form. Error bars = SD (n = 3).

(C and D) Cell extracts were prepared from rescued *atbg1* plants at various time points after dehydration stress and subjected to gel filtration (C). The intensity of the AtBG1:HA band in each fraction was measured from immunoblots. High molecular weight forms ([C], fractions 1 to 7) are presented as a percentage of the total amount of AtBG1:HA (D). Error bars = SD (n = 3).

inhibitory activity from the fractions containing low molecular weight forms (data not shown). These results strongly suggest that the assembly of AtBG1 into high molecular weight forms constitutes the underlying mechanism of activation. Next, we examined the kinetics of AtBG1 assembly into higher molecular weight forms upon dehydration stress. Protein extracts were prepared from rescued *atbg1* plants subjected to dehydration at various time points and fractionated by gel filtration chromatography. The higher molecular weight forms appeared 30 min after dehydration and gradually increased over time (Figures 5C and 5D). At 10 hr after dehydration stress, over 80% of AtBG1 was present in the higher molecular weight form (Figures 5C and 5D). Thus, the assembly of AtBG1 into

higher molecular weight forms upon dehydration stress occurs at a mild condition such as exposure to 30% relative humidity for 30 min, indicating that the response is very sensitive to dehydration stress.

Polymerization of AtBG1 into Higher Molecular Weight Forms Displays Diurnal Fluctuation, Similar to the ABA Level

The water status in plants changes constantly within a day under normal growth conditions. Transpiration rates may reach the highest level at midday under brighter sunlight, which periodically lowers water potential or leads to a transient water deficit at midday. To examine this, we measured the transpiration rate every 6 hr (8:00 AM, 2:00 PM, 8:00 PM, and 2:00 AM) in a day and found that it reaches the highest level at 2:00 PM (Figure S12). Thus, we hypothesized that the ABA levels in leaves undergo diurnal fluctuation, with a higher cellular ABA level at midday and a lower ABA level at night. To test this, we measured the ABA levels in leaves of WT, *atbg1*, and rescued *atbg1* plants grown under normal conditions every 6 hr starting at 8:00 AM. The ABA levels of leaves displayed diurnal fluctuation within a day, with the lowest and highest concentrations at 8:00 AM and 2:00 PM in rescued *atbg1* plants, respectively (Figure 6A and Figure S9C). WT plants also showed a similar ABA pattern. In contrast, the ABA level in *atbg1* plants remained at a basal level without any significant fluctuation, suggesting that AtBG1 plays a major role in diurnal fluctuation of ABA. To investigate the cause of this increase in diurnal fluctuation of ABA, we determined the levels of *AtBG1* transcripts as well as *AtABA1*, *AtABA2*, and *AtNCED3*, which are critical for de novo ABA biosynthesis in WT plants at various time points within a day. Expression of *AtBG1* was induced following dehydration (Figure S2A). Expression of *AtABA2* and *AtNCED3* was also induced by dehydration (Nambara and Marion-Poll, 2005). Furthermore, the *ABA2* mRNA level in *Nicothiana plumbaginifolia* displayed a circadian cycle, although protein expression remained constant (Audran et al., 1998). Under the growth conditions employed, the *AtBG1* and *AtABA2* mRNA levels remained constant throughout a day (Figure S13A), indicating that plants do not experience dehydration stress under these conditions. This result suggests that the higher ABA content was not due to enhanced expression of *AtBG1*. Interestingly, the level of *AtABA1* transcript fluctuated with an approximate 1.7-fold increase at 2:00 PM (Figures S13A and S13B). In addition, *AtNCED3* mRNA expression increased to 1.8-fold at 8:00 PM and remained elevated until 2:00 AM, but returned to the basal level by 8:00 AM. *CCA1* and *TOC1* transcript levels were examined as positive controls for circadian rhythm (Wang and Tobin, 1998; Strayer et al., 2000). *CCA1* and *TOC1* mRNA displayed circadian rhythms, consistent with previous observations (Figures S13C). These results indicate that both *AtABA1* and *AtNCED3* mRNA levels display diurnal fluctuation. However, the degrees of fluctuation of mRNA levels were less than 2-fold. Moreover, the oscillation patterns of these mRNA levels did not overlap with that of ABA levels. These results suggest that de novo synthesis of ABA may not contribute significantly to the rise in ABA levels at 2:00 PM.

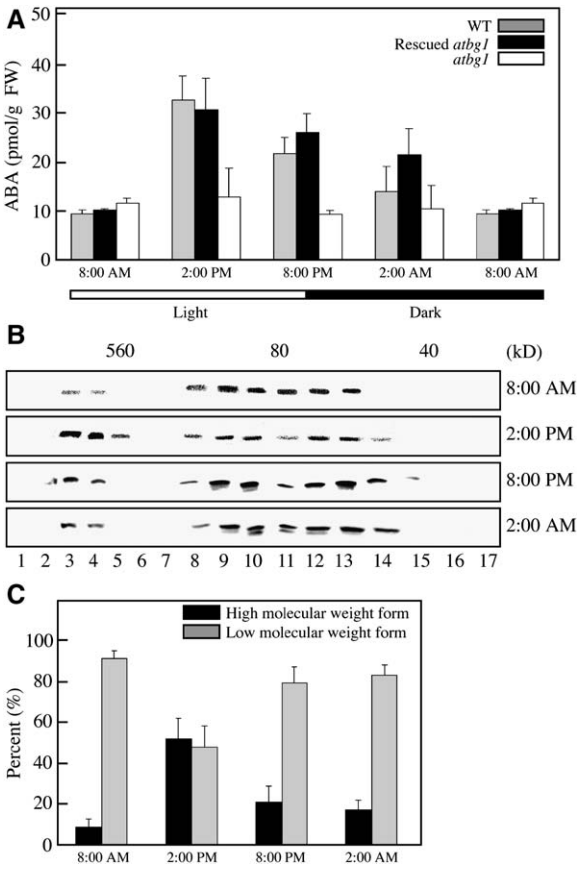

Figure 6. The Amount of the Higher Molecular Weight Forms of AtBG1 Fluctuates Diurnally in Proportion to the ABA Level

(A) The diurnal fluctuation of ABA levels. ABA was measured at the indicated time points from plants (18 days old) grown on soil in a green house under a 12/12 hr light/dark cycle and 70% RH at 20°C. Error bars = SD (n = 3).

(B) Gel filtration analysis of AtBG1:HA in rescued *atbg1* plants throughout a day.

(C) Higher molecular weight AtBG1 (fractions 1 to 6) was quantified, as described in Figure 5D. Error bars = SD (n = 3).

Next, we examined whether AtBG1 contributes to the diurnal fluctuation of ABA levels by the polymerization-mediated activation of AtBG1. Total protein extracts from rescued *atbg1* plants grown under normal conditions at different time points were fractionated using a gel filtration column and analyzed by western blotting using an anti-HA antibody. Interestingly, higher molecular weight AtBG1 showed diurnal fluctuation (Figures 6B and 6C). Levels peaked at 2:00 PM, followed by a rapid decline, and were lowest at 8:00 AM. At 2:00 PM, approximately half the total AtBG1 existed in the higher molecular weight forms, whereas at 8:00 AM, less than 10% high molecular weight AtBG1 was observed. The concentration of high molecular weight AtBG1 correlated significantly with the

increase in ABA content in leaf tissues during the day, strongly suggesting that the polymerization-mediated activation of AtBG1 is responsible for the increased ABA levels during diurnal fluctuation.

ABA Produced by AtBG1 Contributes to the Initiation of Intracellular Signaling as well as to the Increase in the Extracellular ABA Level

Earlier studies show that ABA injected into cells initiates ABA signaling, possibly via an intracellular receptor (Allen et al., 1994; Levchenko et al., 2005). We investigated whether ABA generated by AtBG1 in the ER plays a role in signaling. A chimeric gene, *RD29A-Luc*, comprising *RD29A*, a strong ABA and osmotic stress-inducible promoter (Yamaguchi-Shinozaki and Shinozaki, 1994; Hwang and Sheen, 2001), and the luciferase coding region, was introduced into protoplasts prepared from *atbg1*, WT, and rescued *atbg1* plants. The luciferase activity was measured in these protoplasts (Figure 7A). Luciferase activity in *atbg1* protoplasts was 50% of that of the WT, while that in rescued *atbg1* transgenic plants was 170% of that of WT. The lower level of luciferase activity in *atbg1* protoplasts was restored to the WT level in the presence of transiently coexpressed AtBG1:HA. To obtain independent evidence, the concentration of nitric oxide (NO), a downstream mediator of ABA signaling (Guo et al., 2003), was determined using 4,5-diaminofluorescein diacetate (DAF-2DA). Protoplasts were prepared from plants subjected to dehydration stress in the presence of fluridone, and stained with DAF-2DA to determine the NO content. The fluorescence intensity was significantly stronger in rescued *atbg1* and weaker in *atbg1* protoplasts, compared with WT (Figures 7B and 7C). These findings indicate that ABA produced by AtBG1 in the ER contributes to an increase in intracellular levels for ABA signaling.

ABA exogenously applied to cells initiates signaling (Anderson et al., 1994; Schroeder et al., 2001). We investigated the possibility that ABA generated by AtBG1 might contribute to an increase in extracellular ABA levels. Intracellular and extracellular ABA levels were measured separately for WT and *atbg1* plants (Figure 7D). Although the intracellular ABA level in *atbg1* plants was slightly lower than that in the WT, the extracellular ABA level in *atbg1* plants was 30% of the WT level, indicating that the mutation in *AtBG1* has a marked effect on the extracellular ABA level (Figure 7D). However, ABA and ABA-GE levels in xylem saps were not significantly different between WT and *atbg1* plants (Figure 7E). These results strongly suggest that ABA generated by AtBG1 in the ER is secreted from cells into the apoplastic space of the leaf where it may play a role in initiation of ABA signaling.

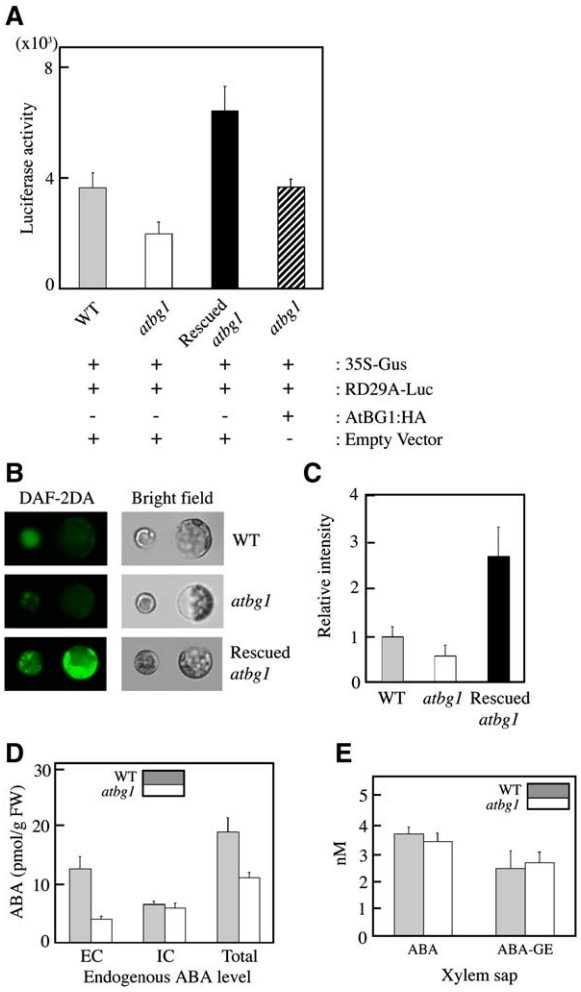

Figure 7. ABA Produced by AtBG1 Contributes to Initiation of Intracellular ABA Signaling as well as to the Increase of the Extracellular ABA Levels

(A) Protein extracts from protoplasts transformed with the indicated constructs were used to measure activities of luciferase and β-glucuronidase. Luciferase activity was normalized, based on the level of β-glucuronidase activity. WT, wild-type. Error bars = SD (n = 3).

(B and C) Nitric oxide levels. Plants were subjected to dehydration stress in the presence of 1.0 μM fluridone. Protoplasts were prepared from plants subjected to stress and stained with DAF-2DA. All images were taken using the same exposure time (B). The intensity was quantified (C). Error bars = SD (n = 50; $p < 0.05$).

(D) ABA was measured in intracellular extracts and extracellular washing fluids as described in the Experimental Procedures. FW, fresh weight. Error bars = SD (n = 3).

(E) ABA and ABA-GE levels in xylem saps were measured as described in the Experimental Procedures. Error bars = SD (n = 3).

DISCUSSION

In this study, we demonstrate that in addition to the de novo ABA biosynthesis (Qin and Zeevaart, 1999; Seo and Koshiba, 2002), the β-glucosidase homolog AtBG1 generates ABA from ABA-GE. Previously, ABA-GE was thought to be biologically inert and to not constitute a stored form (Dietz et al., 2000) although Sauter et al. (2002) suggested that it contributes to homeostasis of ABA. *Arabidopsis* has intracellular and extracellular ABA-GE-hydrolyzing activities, and AtBG1 constitutes the major proportion of intracellular activity (Figure S7) and plays a critical role in the increase of extracellular ABA

levels (Figure 7D). Extracellular ABA-GE hydrolyzing activity was previously reported in barley (Dietz et al., 2000; Sauter et al., 2002). Under dehydration stress conditions, AtBG1 increased the ABA level significantly via two distinct mechanisms: induction of *AtBG1* transcripts and posttranslational activation (Figures S2A and S2C and Figure 5). *AtBG1* expression was detected in most of the seed cells and highly specific to hydathodes in vegetative tissues (Figure S2B). During dehydration stress, *AtBG1* expression was increased in the vasculature of leaves as well as hydathodes (Figure S2C). In addition, AtBG1 enzymatic activity was activated 4-fold by dehydration (Figure 5B) via polymerization to the higher molecular weight forms (Figure 5), which enables plants to accomplish rapid increases in ABA levels in response to dehydration. Furthermore, through the polymerization-mediated activation, AtBG1 contributed to the diurnal increase in ABA levels under normal growth conditions that do not affect *AtBG1* expression (Figure 6 and Figure S13).

The current model indicates that increases in ABA levels occur primarily through de novo biosynthesis under normal and abiotic stress conditions (Seo and Koshiba, 2002; Nambara and Marion-Poll, 2005). Gene encoding enzymes involved in ABA biosynthesis are induced by abiotic stress (Iuchi et al., 2000; Seo et al., 2000), suggesting that de novo synthetic pathways are activated under these conditions to increase ABA levels. In this study, using *atbg1* and rescued *atbg1* plants, we clearly demonstrate that ABA produced by AtBG1 also plays an important role in various physiological responses under normal and abiotic stress conditions. Despite the presence of the intact de novo biosynthetic pathways, *atbg1* plants displayed a variety of ABA-deficient phenotypes, including earlier germination, sensitivity to dehydration stress, and defects in stomatal closure (Figures 1 and 4D), similar to numerous ABA biosynthetic mutants (Marin et al., 1996; Leon-Kloosterziel et al., 1996). In fact, *atbg1* plants display more severe defective phenotypes in growth and ABA-mediated responses than *aba2* plants, which are one of most severe ABA-deficient mutants (Cutler and Krochko, 1999; Seo and Koshiba, 2002) (data not shown). Under dehydration conditions, rescued *atbg1* plants overexpressing AtBG1 accumulated higher levels of ABA than WT plants and displayed enhanced tolerance to dehydration stress (Figures 1G and 1H). These results highlight the importance of AtBG1 in providing the requisite ABA for cellular responses to dehydration stress.

AtBG1 localizes to the ER (Figure 3 and Figure S5), whereas the final steps of de novo synthesis occur in the cytosol (Cutler and Krochko, 1999; Seo and Koshiba, 2002). These findings indicate that ABA is produced in two distinct subcellular locations by two different pathways. Therefore, one possible hypothesis to explain the discrepancy between our data and the current model is that AtBG1 in the ER contributes to the active pool of ABA for rapid physiological responses under normal and stress conditions, whereas ABA synthesized de novo participates in the overall increase in free ABA. De novo ABA biosynthetic pathways, together with ABA glucosyltransferase (Xu et al., 2002), also may contribute to increase in the conjugated ABA levels (Cutler and Krochko, 1999). Consistent with this theory, our results showed that the AtBG1-mediated increase in the ABA level in rescued *atbg1* plants is dependent on the de novo synthesis of ABA (Figure 4C and Figure S10).

The issue of why plants rely on ABA produced from ABA-GE by AtBG1 in response to dehydration stress remains to be resolved. Plants are subjected to ever-changing environmental and physiological conditions, and accordingly, need to constantly fine-tune the active pool of ABA in relation to the severity and duration of stress. Production of ABA from ABA-GE by AtBG1 is just a one-step process, compared with the lengthy and complex de novo biosynthetic pathways. Thus, this pathway is ideal for rapid increase of the ABA content necessary for plants to meet physiological needs. Another elegant mechanism is the rapid activation of AtBG1 through dehydration-induced polymerization, which enables plants to increase ABA levels robustly in a short time under dehydration conditions (Figure 5). Furthermore, plants use AtBG1 to adjust the active pool of ABA for physiological responses without activating dehydration signaling, as demonstrated by the data showing that polymerization-mediated AtBG1 activation is responsible for diurnal increases in ABA levels under normal growth conditions (Figure 6 and Figure S13).

In plant leaves, ABA-GE is stored in the vacuole and apoplastic space (Dietz et al., 2000), whereas AtBG1 is localized to the ER (Figure 3 and Figure S5). One possible explanation is that AtBG1 and its substrate are stored separately in the cell, and only brought together when cells need to increase the ABA content, as in the case of abiotic stress conditions (Qin and Zeevaart, 1999; Cutler and Krochko, 1999). In this situation, the amount of ABA produced by AtBG1 may be controlled precisely and rapidly to meet plant requirements. Indeed, overexpression of AtBG1 per se increased the endogenous ABA level only slightly in both leaves and roots (Figure 4C and Figure S10). In contrast, the ABA content increased 20-fold under dehydration conditions (Figure 4C). The enhanced ABA content in plant cells correlated directly with the higher ABA production ability of AtBG1 in the ER (Figure 3D), suggesting that dehydration stress acts as a signal to transport ABA-GE stored in the vacuole or apoplastic space to the ER. Consistent with this hypothesis, we observed that ABA-GE is actively imported into the ER via the ER membrane (Figure 3C). It would be interesting to identify the transporters responsible for ABA-GE transport. Thus, under dehydration conditions, the amount of ABA-GE supplied for AtBG1 in the ER lumen may be increased. Dehydration-induced activation of both AtBG1 and the putative transporter in the ER membrane may result in rapid production of ABA from ABA-GE within a brief time.

Another important issue that needs to be resolved is the site of action of ABA produced by AtBG1 in plant cells. Our results demonstrated that ABA generated by AtBG1 in the ER contributes to ABA-mediated signaling in at least two

different ways. One way is through the increase in the intracellular ABA. This conclusion is based on two lines of evidence; the expression of the *luciferase* reporter gene under the control of the *RD29A* promoter (Yamaguchi-Shinozaki and Shinozaki, 1994; Hwang and Sheen, 2001) was increased by transiently expressed AtBG1 in protoplasts (Figure 7A), and the levels of NO, a downstream mediator of ABA, were respectively lower and higher in *atbg1* and rescued *atbg1* protoplasts, compared with the WT (Figures 7B and 7C). This is consistent with previous studies showing that intracellular ABA initiates ABA-mediated signaling (Allen et al., 1994; Levchenko et al., 2005). The other way ABA generated by AtBG1 in the ER contributes to ABA-mediated signaling is through the increase in extracellular ABA levels, as observed previously (Anderson et al., 1994; Schroeder et al., 2001). This is based on data showing that the extracellular ABA level in *atbg1* plants was 30% of the WT level (Figure 7D). Thus, ABA generated by AtBG1 in the ER is probably secreted into the extracellular space where it may contribute to ABA signaling locally. It could also diffuse to neighboring cells through the apoplastic space. However, ABA generated in the ER by AtBG1 may not be transported to other tissues over long distance through the xylem system in the absence of stress (Figure 7E).

EXPERIMENTAL PROCEDURES

Growth of Plants

Unless specified otherwise, *Arabidopsis* plants (ecotype Columbia) were grown either on MS plates at 20°C in a culture room or in soil in a greenhouse under a condition of 70% relative humidity (RH) and a 16/8 hr light/dark cycle at 20°C–23°C.

Assay of AtBG1 Activity In Vitro

Cell extracts from transformed protoplasts were prepared as described previously (Jin et al., 2001). Immunopurification of AtBG1:HA using an anti-HA antibody was performed as described previously (Cutler, 2004). Immunopurified AtBG1:HA proteins were incubated with ABA-GE (1 nmol) (Apex Organics LTD, Devon, UK) in 1.0 ml of 100 mM citrate buffer (pH 5.5) for 1.5 hr at 37°C, and the reaction products were separated by HPLC using a prepacked RT 250-4 column (MERCK) containing 40% methanol, 0.1 M acetic acid, and 10 mg/L butylated hydroxytoluene as the solvent.

To assay ABA-GE hydrolyzing activity from microsomes, protoplasts were prepared from leaf tissues of rescued *atbg1* plants and transformed with *AtERD2:GFP* (Takeuchi et al., 2000). Transformed protoplasts were homogenized in lysis buffer (25 mM HEPES [pH 7.0], 250 mM sucrose, 10 mM $MgCl_2$, 1 mM DTT), and centrifuged at 10,000 g at 4°C for 5 min to remove debris. Homogenates were separated into supernatant and pellet (microsomal) fractions by ultracentrifugation at 100,000 g at 4°C for 1 hr. The microsomal fraction was resuspended in lysis buffer and further treated with thermolysin (10 μg/mL) or Triton X-100 (1%) on ice for 30 min. Samples were diluted 10-fold with lysis buffer and used to assay ABA-GE hydrolyzing activity in 1.0 ml lysis buffer with 100 pmol ABA-GE at 37°C for 1 hr. The activity was normalized by the total amount of microsomal proteins determined by the Bradford solution.

Measurement of Endogenous ABA and ABA-GE

Seed, leaf, and root tissues ground in liquid nitrogen were extracted with 80% methanol at 4°C for 3 hr. The methanol extracts were centrifuged at 3000 g for 10 min to remove debris and freeze-dried at −70°C. The powder was dissolved in TBS buffer (25 mM Tris-HCl [pH 7.5], 100 mM NaCl, 0.1 mM $MgCl_2$, 0.3% NaN_3) and fractionated by HPLC equipped with a C18 column (J.T. Baker, Phillipsburg, NJ) (Ali-Rachedi et al., 2004). The peak corresponding to ABA was quantified by ELISA with an anti-ABA antibody in accordance with the manufacturer's protocol (Banowetz et al., 1994). The extracellular washing fluids were prepared as described previously (Dietz et al., 2000). Details for harvest of xylem sap of *Arabidopsis* to measure ABA and ABA-GE are described in the Supplemental Experimental Procedures.

Localization of AtBG1:HA and Endo H and PNGase F Treatment

Localization and endo H treatment were carried out as described previously (Park et al., 2004). Details are described in the Supplemental Experimental Procedures.

Fractionation of AtBG1 Using Gel Filtration Column Chromatography

To fractionate AtBG1:HA from rescued *atbg1* plants, leaf tissues were homogenized in grinding buffer (50 mM sodium phosphate [pH 7.0], 0.15 M NaCl, 0.02% NaN_3, 1.0 mM DTT, 0.1% Triton X-100). Homogenates were centrifuged at 14,000 g for 5 min to remove debris, and the supernatant was applied to a Sephacryl S-300 high-resolution column. Proteins were eluted using the homogenization buffer without Triton X-100 at a flow rate of 0.5 ml/min in a fraction volume of 3.0 ml. Fractions were analyzed by western blotting using an anti-HA antibody.

Supplemental Data

The Supplemental Data for this article can be found online at http://www.cell.com/cgi/content/full/126/6/1109/DC1/.

ACKNOWLEDGMENTS

This work was supported by a grant to I.H. from a national creative research program from the Ministry of Science and Technology (Korea), and, in part, by grants to I.H., from the Plant Diversity Research Center of the Ministry of Science and Technology (Korea); J.M.K., from the National Research Initiative of the USDA Cooperative State Research Education and Extension Service (2004-35100-14909); and W.H. and F.J., by Deutsche Forschungsgemeinschaft (SFB 567, A6).

Received: November 9, 2005
Revised: February 20, 2006
Accepted: July 19, 2006
Published: September 21, 2006

REFERENCES

Ali-Rachedi, S., Boinot, D., Wagner, M.-H., Bonnet, M., Sotta, B., Grappin, P., and Jullien, M. (2004). Changes in endogenous abscisic acid levels during dormancy release and maintenance of mature seeds: studies with the Cape Verde Islands ecotype, the dormant model of *Arabidopsis thaliana*. Planta *219*, 479–499.

Allen, A.C., Fricker, M.D., Ward, J.L., Beale, M.H., and Trewavas, A.J. (1994). Two transduction pathways mediate rapid effects of abscisic acid in Commelina guard cells. Plant Cell *6*, 1319–1328.

Anderson, B.E., Ward, J.M., and Schroeder, J.I. (1994). Evidence for an extracellular reception site for abscisic acid in Commelina guard cells. Plant Physiol. *104*, 1177–1183.

Audran, C., Borel, C., Frey, A., Sotta, B., Meyer, C., Simonneau, T., and Marion-Poll, A. (1998). Expression studies of the zeaxanthin epoxidase gene in nicotiana plumbaginifolia. Plant Physiol. *118*, 1021–1028.

Baier, M., Gimmler, H., and Hartung, W. (1988). Permeability of the guard cell plasmamembrane and tonoplast. J. Exp. Bot. *41*, 351–358.

Banowetz, G.M., Hess, J.R., and Carman, J.G. (1994). A monoclonal antibody against the plant growth regulator, abscisic acid. Hybridoma *13*, 537–541.

Chiwocha, S.D., Cutler, A.J., Abrams, S.R., Ambrose, S.J., Yang, J., Ross, A.R., and Kermode, A.R. (2005). The etr1-2 mutation in Arabidopsis thaliana affects the abscisic acid, auxin, cytokinin and gibberellin metabolic pathways during maintenance of seed dormancy, moist-chilling and germination. Plant J. *42*, 35–48.

Cutler, A.J., and Krochko, J.E. (1999). Formation and breakdown of ABA. Trends Plant Sci. *4*, 472–478.

Cutler, P. (2004). Immunoaffinity chromatography. Methods Mol. Biol. *244*, 167–177.

Dietz, K.-J., Sauter, A., Wichert, K., Messdaghi, D., and Hartung, W. (2000). Extracellular β-glucosidase activity in barley involved in the hydrolysis of ABA glucose conjugate in leaves. J. Exp. Bot. *51*, 937–944.

Gamble, P.E., and Mullet, J.E. (1986). Inhibition of carotenoid accumulation and abscisic acid biosynthesis in fluridone-treated dark-grown barley. Eur. J. Biochem. *160*, 117–121.

Guo, F.-Q., Okamoto, M., and Crawford, N.M. (2003). Identification of a plant nitric oxide synthase gene involved in hormonal signaling. Science *302*, 100–103.

Hartung, W., Sauter, A., and Hose, E. (2002). Abscisic acid in the xylem: where does it come from, where does it go to? J. Exp. Bot. *53*, 27–32.

Himmelbach, A., Yang, Y., and Grill, E. (2003). Relay and control of abscisic acid signaling. Curr. Opin. Plant Biol. *6*, 470–479.

Hwang, I., and Sheen, J. (2001). Two-component circuitry in Arabidopsis cytokinin signal transduction. Nature *413*, 383–389.

Iuchi, S., Kobayashi, M., Yamaguchi-Shinozaki, K., and Shinozaki, K. (2000). A stress-inducible gene for 9-cis-epoxycarotenoid dioxygenase involved in abscisic acid biosynthesis under water stress in drought-tolerant cowpea. Plant Physiol. *123*, 553–562.

Jin, J.B., Kim, Y.A., Kim, S.J., Lee, S.H., Kim, D.H., Cheong, G.W., and Hwang, I. (2001). A new dynamin-like protein, ADL6, is involved in trafficking from the trans-Golgi network to the central vacuole in Arabidopsis. Plant Cell *13*, 1511–1526.

Kim, Y.-W., and Kim, I.S. (1998). Subunit composition and oligomer stability of oat beta-glucosidase isozymes. Biochim. Biophys. Acta *1388*, 457–464.

Kushiro, T., Okamoto, M., Nakabayashi, K., Yamagishi, K., Kitamura, S., Asami, T., Hirai, N., Koshiba, T., Kamiya, Y., and Nambara, E. (2004). The Arabidopsis cytochrome P450 CYP707A encodes ABA 8′-hydroxylases: key enzymes in ABA catabolism. EMBO J. *23*, 1647–1656.

Kuznetsov, G., Brostrom, M.A., and Brostrom, C.O. (1993). Role of endoplasmic reticular calcium in oligosaccharide processing of alpha 1-antitrypsin. J. Biol. Chem. *268*, 2001–2008.

Leon-Kloosterziel, K.M., van de Bunt, G.A., Zeevaart, J.A., and Koornneef, M. (1996). Arabidopsis mutants with a reduced seed dormancy. Plant Physiol. *110*, 233–240.

Levchenko, V., Konrad, K.R., Dietrich, P., Roelfsema, M.R., and Hedrich, R. (2005). Cytosolic abscisic acid activates guard cell anion channels without preceding Ca^{2+} signals. Proc. Natl. Acad. Sci. USA *102*, 4203–4208.

Marana, S.R., Jacobs-Lorena, M., Terra, W.R., and Ferreira, C. (2001). Amino acid residues involved in substrate binding and catalysis in an insect digestive beta-glycosidase. Biochim. Biophys. Acta *1545*, 41–52.

Marin, E., Nussaume, L., Quesada, A., Gonneau, M., Sotta, B., Hugueney, P., Frey, A., and Marion-Poll, A. (1996). Molecular identification of zeaxanthin epoxidase of Nicotiana plumbaginifolia, a gene involved in abscisic acid biosynthesis and corresponding to the ABA locus of Arabidopsis thaliana. EMBO J. *15*, 2331–2342.

Munro, S., and Pelham, H.R. (1987). A C-terminal signal prevents secretion of luminal ER proteins. Cell *48*, 899–907.

Nambara, E., and Marion-Poll, A. (2005). Abscisic acid biosynthesis and catabolism. Annu. Rev. Plant Biol. *56*, 165–185.

Park, M., Kim, S.J., Vitale, A., and Hwang, I. (2004). Identification of the protein storage vacuole and protein targeting to the vacuole in leaf cells of three plant species. Plant Physiol. *134*, 625–639.

Pih, K.T., Jang, H.J., Kang, S.G., Piao, H.L., and Hwang, I. (1997). Isolation of molecular markers for salt stress responses in Arabidopsis thaliana. Mol. Cells *7*, 567–571.

Qin, X., and Zeevaart, J.A. (1999). The 9-cis-epoxycarotenoid cleavage reaction is the key regulatory step of abscisic acid biosynthesis in water-stressed bean. Proc. Natl. Acad. Sci. USA *96*, 15354–15361.

Rock, C.D., and Zeevaart, J.A. (1991). The aba mutant of Arabidopsis thaliana is impaired in epoxy-carotenoid biosynthesis. Proc. Natl. Acad. Sci. USA *88*, 7496–7499.

Sauter, A., Dietz, K.J., and Hartung, W. (2002). A possible stress physiological role of abscisic acid conjugates in root-to-shoot signalling. Plant Cell Environ. *25*, 223–228.

Schroeder, J.I., Allen, G.J., Hugouvieux, V., Kwak, J.M., and Waner, D. (2001). Guard cell signal transduction. Annu. Rev. Plant Physiol. Plant Mol. Biol. *52*, 627–658.

Seo, M., and Koshiba, T. (2002). Complex regulation of ABA biosynthesis in plants. Trends Plant Sci. *7*, 41–48.

Seo, M., Koiwai, H., Akaba, S., Komano, T., Oritani, T., Kamiya, Y., and Koshiba, T. (2000). Abscisic aldehyde oxidase in leaves of Arabidopsis thaliana. Plant J. *23*, 481–488.

Shinozaki, K., and Yamaguchi-Shinozaki, K. (2000). Molecular responses to dehydration and low temperature: differences and cross-talk between two stress signaling pathways. Curr. Opin. Plant Biol. *3*, 217–223.

Strayer, C., Oyama, T., Schultz, T.F., Raman, R., Somers, D.E., Mas, P., Panda, S., Kreps, J.A., and Kay, S.A. (2000). Cloning of the Arabidopsis clock gene TOC1, an autoregulatory response regulator homolog. Science *289*, 768–771.

Takeuchi, M., Ueda, T., Sato, K., Abe, H., Nagata, T., and Nakano, A. (2000). A dominant negative mutant of sar1 GTPase inhibits protein transport from the endoplasmic reticulum to the Golgi apparatus in tobacco and Arabidopsis cultured cells. Plant J. *23*, 517–525.

Tan, B.C., Schwartz, S.H., Zeevaart, J.A., and McCarty, D.R. (1997). Genetic control of abscisic acid biosynthesis in maize. Proc. Natl. Acad. Sci. USA *94*, 12235–12240.

Wang, Z.Y., and Tobin, E.M. (1998). Constitutive expression of the *CIRCADIAN CLOCK ASSOCIATED 1* (*CCA1*) gene disrupts circadian rhythms and suppresses its own expression. Cell *93*, 1207–1217.

Wilkinson, S., and Davies, W.J. (2002). ABA-based chemical signalling: the co-ordination of responses to stress in plants. Plant Cell Environ. *25*, 195–210.

Xu, Z.J., Nakajima, M., Suzuki, Y., and Yamaguchi, I. (2002). Cloning and characterization of the abscisic acid-specific glucosyltransferase gene from adzuki bean seedlings. Plant Physiol. *129*, 1285–1295.

Yamaguchi-Shinozaki, K., and Shinozaki, K. (1994). A novel cis-acting element in an Arabidopsis gene is involved in responsiveness to drought, low-temperature, or high-salt stress. Plant Cell *6*, 251–264.

Zeevaart, J.D.A. (1999). Abscisic acid metabolism and its regulation. In Biochemistry and Molecular Biology of Plant Hormones, P.J.J. Hooykaas, M.A.K. Hall, and R. Libbenga, eds. (Amsterdam: Elsevier), pp. 189–207.

Zhu, J.K. (2002). Salt and drought stress signal transduction in plants. Annu. Rev. Plant Biol. *53*, 247–273.